An alternative phase modulator half-wave voltage measurement based on photonic link

Quanyi Ye (叶全意), Chun Yang (杨 春)*, Yuhua Chong (崇毓华), and Xianghua Li (李向华)

School of Electronic Science and Engineering, Southeast University, Nanjing 210096, China

**Corresponding author: yangchun_seu@163.com*

Received January 26, 2013; accepted April 3, 2013; posted online July 3, 2013

We measure the half-wave voltage of $LiNbO_3$ phase modulators in a 26-GHz wideband frequency range, and then analyze it by the phase modulation photonic peak gain linked to the interferometric demodulation. The optical interferometer is constructed with two 50:50 couplers and two fiber arms with a 1-m difference in fiber length. The photonic link gain peaks are frequency dependent, as indicated by the differential time delay in the interferometer. The procedure described is a new and practical half-wave voltage measurement method that can accurately predict the nonlinear frequency characteristics of the phase modulator. Moreover, the method can be applied to various types of $LiNbO_3$ phase modulators.

OCIS codes: 120.5060, 230.4110, 060.2360.

doi: 10.3788/COL201311.071202.

Due to its advantageous characteristics, including low loss, small size, large bandwidth, and superior stability and immunity to external interference, the photonic link has been considered in various applications, such as standard frequency distribution networks, remote sensing, radar systems, and communication systems[1-3]. External intensity modulation with direct detection is traditionally used in transmitting signals through fiber. However, the great potential of the phase modulation photonic link has been proven in recent applications; the method eliminates the bias circuit and provides a more linear optical phase conversion of input voltage[4-7].

The half-wave voltage (V_π) is the voltage required to produce a π radians phase shift, which influences the performance of analogue photonic links[8]. One typical method uses an optical spectrum analyzer to observe the intensity ratio of the modulated optical side bands[8,9]. Such method entails carrier nulling and multiple sideband ratio procedures, which require a significantly high driving voltage[8]. The high driving voltage may change the optoelectronic properties of a modulator, and this overdrive may damage the device being tested. Another method is to convert output intensity variations into an electrical signal with a photodiode, and the resulting signal can be measured using a microwave spectrum analyzer[10,11]. However, these methods are limited by the bandwidth of the measuring instruments and the linewidth of the optical sources. Moreover, point-by-point measurements for a full investigation of the frequency behavior are performed slowly.

In this letter, we propose an alternative method to measure the half-wave voltage of $LiNbO_3$ phase modulators based on the phase modulation photonic link peak gain. Our presentation describes the analysis of features in detail. We then apply this method to characterize the half-wave voltage of $LiNbO_3$ phase modulator up to 26 GHz. The experimental procedures and results show that this broadband half-wave voltage measurement has a simple structure and is easy to operate.

The schematic diagram of the half-wave voltage measurement system is shown in Fig. 1. The light wave, which is phase-modulated, is divided into a simple nonbalanced Mach–Zehnder interferometer (MZI) (comprising two 3-dB couplers with 1-m fiber length difference). The FM–AM transformed signal is converted back into the electrical domain by the photodiode at the link output.

The photocurrent output of the photodiode is given by[12]

$$I(t) = I_{\rm dc}\{1+\sin[\varphi(t-\tau)-\varphi(t)]\}, \tag{1}$$

where $I_{\rm dc} = \Re\alpha P_{\rm in}/2$ is the DC current from the photodiode, with $\Re$ as the photodiode responsivity and α as the total photonic link loss; $\varphi(t) = V_{\rm RF}\sin(\omega_{\rm RF}t)/2V_\pi$ with $V_{\rm RF}\sin(\omega_{\rm RF}t)$ as the driving signal, V_π as the half-wave voltage of the phase modulator, and τ as the MZI differential time delay. Using the small signal model ($V_{\rm RF}/V_\pi \ll 1$), we expand Eq. (1) with the Bessel function of the first kind to obtain the RF output power given as

$$\begin{aligned} I_{\rm RF}(t)=&\tfrac{1}{2}I_{\rm dc}\Big\{\Big\{-2\sum_{n=1}^{\infty}J_{2n-1}(\tfrac{\pi V_{\rm RF}}{V_\pi})[\cos(2n-1)\omega_{\rm RF}(t-\tau)]\Big\}\Big\{J_0(\tfrac{\pi V_{\rm RF}}{V_\pi})+2\sum_{n=1}^{\infty}J_{2n}(\tfrac{\pi V_{\rm RF}}{V_\pi})[\cos(2n)\omega_{\rm RF}(t)]\Big\}\\ &-\Big\{J_0(\tfrac{\pi V_{\rm RF}}{V_\pi})+2\sum_{n=1}^{\infty}J_{2n}(\tfrac{\pi V_{\rm RF}}{V_\pi})[\cos(2n)\omega_{\rm RF}(t-\tau)]\Big\}\Big\{-2\sum_{n=1}^{\infty}J_{2n-1}(\tfrac{\pi V_{\rm RF}}{V_\pi})[\cos(2n-1)\omega_{\rm RF}(t)]\Big\}\Big\}, \end{aligned} \tag{2}$$

where J_n is the nth order Bessel function. The output power at the fundamental frequency can be written as

$$P_{\rm RF\_out} = 2I_{\rm dc}^2J_0^2\left(\frac{\pi V_{\rm RF}}{V_\pi}\right)J_1^2\left(\frac{\pi V_{\rm RF}}{V_\pi}\right)\sin^2\omega_{\rm RF}\left(\frac{\tau}{2}\right)Z_{\rm out}. \tag{3}$$

From Eq. (3), we can calculate the small-signal gain for phase modulation photonic link using

$$G_{\rm RF} = \left[\frac{2I_{\rm dc}\pi}{V_\pi}\sin(\frac{\tau}{2}\omega_{\rm RF})\right]^2 Z_{\rm in}Z_{\rm out}, \tag{4}$$

where $Z_{\rm in}$ and $Z_{\rm out}$ are the load resistances. Equation (4) predicts the frequency-dependent gain peaks and demonstrates a limiting factor of the photonic link.

Figure 2 shows the normalized gain as a function of frequency with differential delay times of 200, 100, and 50 ps. The gain peaks for a phase modulation optical link given at the special frequency ($\sin^2(\omega_{\rm RF}\tau/2) = 1$) can be calculated as

$$G_{\rm RF\_peak} = \left(\frac{2I_{\rm dc}\pi}{V_\pi}\right)^2 Z_{\rm in}Z_{\rm out}. \quad (5)$$

From Eq. (5), the link gain peak is observed to be inversely proportional to the square of the half-wave voltage. Thus, the half-wave voltage of the $LiNbO_3$ phase modulator is

$$V_\pi = 2I_{\rm dc}\pi\sqrt{\frac{Z_{\rm in}Z_{\rm out}}{G_{\rm RF\_peak}}}. \quad (6)$$

This equation is a concise analytical expression showing the phase modulator half-wave voltage, and the model can be expressed easily without the harmonic terms. From Eq. (6), we can observe that if the total DC current $I_{\rm dc}$, photodiode responsivity $\Re$, and $Z_{\rm in}Z_{\rm out}$ are kept constant, the half-wave voltage of the phase modulator is the only peak gain function $G_{\rm peak}$. This function can be calculated directly from the different frequency signal levels using a vector network analyzer.

In the present experiments, photonic link gain is measured using an Agilent vector network analyzer (N5242A). Based on the system configuration (Fig. 1) and the theoretical concepts, a laser with a center wavelength of 1550 nm is used with an input optical power of 16 dBm. The inset in Fig. 3 shows the measured photonic link gain curve. The gain peak is about –15.13 dB at 0.1 GHz and –16.77 dB at 0.3 GHz. The free spectral range (FSR) of the gain is 200 MHz, obtained at the optimum input signal. To our knowledge, Fig. 3 represents 130 gain peaks in the photonic link, as measured by the 26-GHz Agilent vector network analyzer. The gain follows a downward trend as the frequency increases, mainly due to the frequency response of the phase modulator and the photodiode.

In our experiments, the total photonic link attenuation is 4 dB, the photodiode responsivity is 0.85 A/W, and the DC current $I_{\rm dc} = \Re a P_{\rm in}/2 = 6.7$ mA. Figure 4 shows the half-wave voltage as a function of frequency, calculated using Eq. (6). The measured data (black line) is higher than the calibration data of the photodiode frequency responses (red line) because the frequency response of the photodiode has an important function in deciding the photonic link gain. The effective half-wave voltage of the phase modulator increases with frequency, starting from 3.8 V at DC, 4.6 V at 1 GHz, until 9.7 V at 26 GHz is reached. At a frequency range of 0−10 GHz, the half-wave voltage is less than 7 V. In the 10−20 GHz range, the half-wave voltage is almost constant with a value of approximately 7 V. After 20 GHz, the half-wave voltage increases rapidly, with a maximum value greater than 10 V at 24.5 GHz.

From Eq. (4), the gain peaks for the optical link can be generated at the special frequency ($\sin^2(\omega_{\rm RF}\tau/2) = 1$). The FSR of the photonic link is $1/\tau$. Thus, the number of gain peaks, $N = F/{\rm FSR} = Fn\Delta L/c$, is actually proportional to the MZI differential delay time. F is the vector network analyzer bandwidth, ΔL is the difference in the fiber lengths of the two MZI arms, n is the refractive index of the fiber, and c is the light speed 3×10^8 m/s. Higher accuracy is obtained for the phase modulator half-wave voltage when the length difference of the MZI arms is larger.

As expected from the discussion above, the half-wave voltage of phase modulator measured data with optical spectrum analysis (OSA) method as Ref. [8] and our method is obtained. The two results are plotted in Fig. 5 showing that the half-wave voltage of phase modulator is in consistence with data using our method. However, using OSA method can only measure the frequency response of phase modulator in 11-GHz frequency while the driving microwave signal is less than 30 dBm and the point-by-point measurements are slow for a full investigation of the frequency behavior. The measured phase modulator data are applied to a 5-GHz signal transmission photonic link, and the delay time difference of MZI is 100 ps. In our experiments, the input optical power is 10.5 dBm, the total photonic

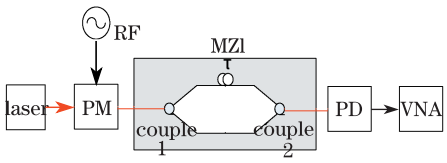

Fig. 1. Configuration of the half-wave voltage measurement system based on the photonic link. PM: phase modulator; PD: photodiode; VNC: vector network analyzer.

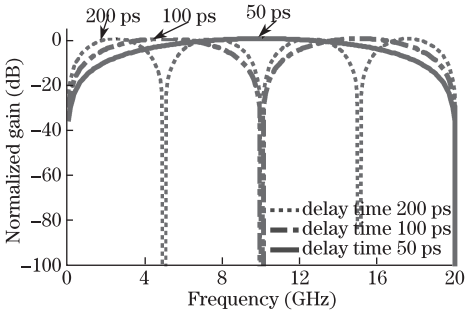

Fig. 2. Normalized gain as a function of frequency with differential MZI delay times of 200, 100, and 50 ps.

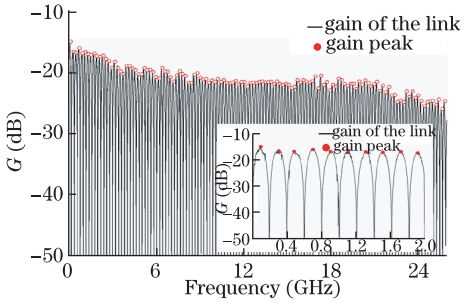

Fig. 3. Photonic link gain curve measured with a 26-GHz Agilent vector network analyzer with an FSR=200 MHz. The inset shows the photonic link gain peaks at 2-GHz frequency range.

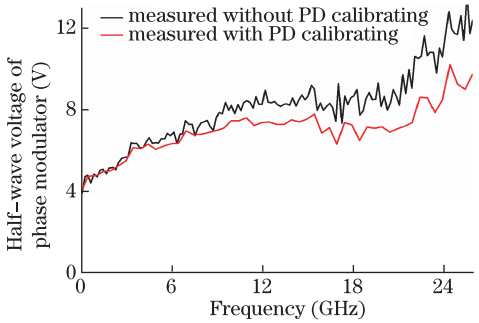

Fig. 4. (Color online) Half-wave voltage curve of the phase modulator measured with (red line) and without (black line) the calibrated photodiode frequency responses.

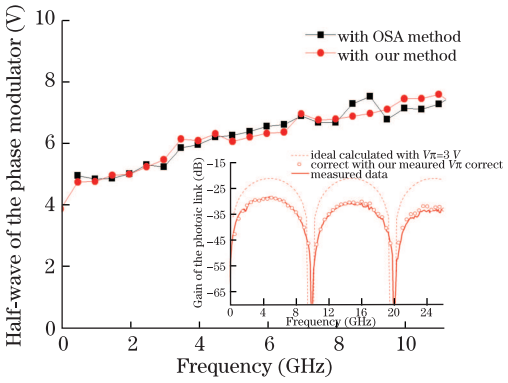

Fig. 5. (Color online) Measured half-wave voltage of phase modulator measured data (black line) with OSA method and those data (red line) with our method. The inset represents the measured (solid line) and ideal link gain with Eq. (4) (dotted line), and calculated data (circle dots) with our measured half-wave voltage frequency response.

link attenuation is 6 dBm, the photodiode responsivity is 0.7 A/W, and the DC current $I_{\rm dc} = \Re a P_{\rm in}/2 = 1\,{\rm mA}$. Figure 5 shows the link gain plots as a function of modulation frequency. The solid and dotted lines are the experimental and theoretical values of Eq. (4) obtained using a 3-V phase modulator half-wave voltage. The circle dotted line represent the data obtained after correcting the frequency response of the phase modulator in Fig. 3. The gain peaks are –27.4 dB at 5, 15, and 25 GHz, whereas the half-wave voltage of the phase modulator is 3 V. However, the measured gain peaks are –28.8 dB at 5 GHz, –31.4 dB at 15 GHz, and –34 dB at 25 GHz. Comparing the measured (solid line) and theoretical values with the corrected data (circle dotted line), both are observed to be in good agreement to the latter. This result also proves the effectiveness of this measuring method for the half-wave voltage of $LiNbO_3$ phase modulators.

In conclusion, we measure the phase modulator frequency response at a 26-GHz frequency range using the phase modulation photonic link. This method has a simple structure and can be easily operated. The technique described above has potential significant applications in phase modulators. We believe that accurate characterization of phase modulation parameters is important in developing high-performance photonic links. Numerous extensions of this work are suggested, including detailed error analysis using conventional methods.

This work was supported by the Chinese Defense Advance Research Program of Science and Technology, China under Grant No. 6906005003.

References

1. S. Montebugnoli, M. Boschi, F. Perini, P. Faccin, G Brunori, and E Pirazzini, Microw. Opt. Technol. Lett. **46,** 48 (2005).
2. J. F. Diehl, V. J. Urick, C. S. McDermitt, F. Bucholtz, P. S. Devgan, and K. J. Williams, IEEE Trans. Microw. Theory Technol. **60,** 195 (2012).
3. W. M. Dorsey, C. S. McDermitt, F. Bucholtz, and M. G. Parent, IEEE Trans. Antenn. Propag. **58,** 5288 (2010).
4. L. Liu, S. Zheng, X. Zhang, X. Jin, and H. Chi, J. Electromagn. Waves Appl. **24,** 123 (2010).
5. B. Wang, Z. Li, and X. Wang, Chin. Opt. Lett. **10,** 071202 (2012).
6. B. M. Haas and T. E. Murphy, IEEE Photon. Technol. Lett. **19,** 729 (2007).
7. S. Zou, Y. Wang, Y. Shao, J. Zhang, J. Yu, and N. Chi, Chin. Opt. Lett. **10,** 070625 (2012).
8. Y. Shi, L. Yan, and A. E. Willner, J. Lightwave Technol. **21,** 2358 (2003).
9. L.-S. Yan, A. E. Willner, and Y. Shi, IEEE Photon. Technol. Lett. **17,** 1486 (2005).
10. E. H. W. Chan and R. A. Minasian, J. Lightwave Technol. **26,** 2882 (2008).
11. S. Zhang, X. Zhang, and Y. Liu, Chin. Phys. Lett. **29,** 084217 (2012).
12. V. J. Urick, F. Bucholtz, J. D. McKinney, P. S. Devgan, A. L. Campillo, J. L. Dexter, and K. J. Williams, IEEE Trans. Microw. Theory Technol. **55,** 1978 (2007).